

Supporting Information

Importance of Functional Group in Cross-linking Methoxysilane Additives for High Efficiency and Stable Perovskite Solar Cells

Lin Xie,^{1a,c} Jiangzhao Chen,^{1a} Parth Vashishtha^b, Xing Zhao^a, Gwang Su Shin^a,
Subodh G. Mhaisalkar^{*bc} and Nam-Gyu Park^{*a}

^a School of Chemical Engineering, Sungkyunkwan University, Suwon 440-746, Korea

^b School of Materials Science and Engineering, Nanyang Technological University (NTU), 50 Nanyang Avenue, Singapore 639798, Singapore

^c Energy Research Institute @ Nanyang Technological University (NTU) (ERI@N), Research Techno Plaza, X-Frontier Block, Level 5, 50 Nanyang Drive, Singapore 637553.

Experimental

Material synthesis. Formamidium iodide (FAI) was synthesized by reacting 60 mL HI (57 wt% in water, TCI) with 30 g formamidinium acetate (99%, Aldrich) in an ice bath. After stirring for 3 h, the precipitate was recovered using a rotary evaporator at 60 °C for 1 h and the resulting precipitate was washed with diethyl ether (99.0%, SAMCHUN) to get white powder. The white powder was recrystallized in anhydrous ethanol, which was washed with diethyl ether three times and then dried in vacuum oven at 60 °C for 24 h. The methylammonium bromide (MABr) and methylammonium chloride (MACl) were synthesized by reacting 1 M methylamine (99%, Alfa Aesar) with 1.5 M HBr (48% aqueous solution, Alfa Aesar) and HCl (37% aqueous solution, TCI), respectively. The synthetic procedure for MABr and MACl was the same as that for FAI.

Device fabrication. Fluorine-doped tin oxide (FTO) coated glass substrates (Pilkington,

TEC-8, $8 \Omega \text{ sq}^{-1}$) were ultrasonically cleaned with deionized water, acetone and 2-propanol for 15 min. The cleaned substrates were dried in the vacuum oven for 15 min, which was followed by UV-ozone treatment for 20 min. A tin (IV) oxide (SnO_2) compact layer was formed on top of FTO involves a chemical bath deposition (CBD) method as follows. 1.05 g of urea was dissolved in 840 ml deionized water, which was followed by the addition of 21 μL mercaptoacetic acid and 1.05 mL HCl (37% aqueous solution). Finally, 0.21 g $\text{SnCl}_2 \cdot 2\text{H}_2\text{O}$ (Sigma-Aldrich, >99.995%) was added to the solution and then the solution was sonicated for 5 min. The UV ozone treated FTO substrates were horizontally laid in a glass container filled with the SnCl_2 solution and heated at 70 °C in a lab oven for 3 h, which was followed by heat-treatment with a lid at 180 °C for 1 h in ambient air to form SnO_2 compact layer. The SnO_2 coated FTO substrate was treated again with UV-Ozone for 20 min prior to deposition of perovskite film. The PbI_2 precursor solution was prepared by dissolving 1.5 M lead (II) iodide (PbI_2 , TCI, 99.99%) in 1 mL N,N-dimethylformamide (DMF, Sigma-Aldrich, anhydrous, 99.8%), which contained 100 μL dimethyl sulfoxide (DMSO, Sigma-Aldrich, anhydrous, 99.9%). The PbI_2 solution was stored at 65 °C in N_2 filled glove box overnight before spin-coating. For addition of cross-linking agent in the PbI_2 solution, 17.5 mmol 3-cyanopropyltriethoxysilane (CPTS, 98%, Sigma-Aldrich), (3-mercaptopropyl)trimethoxysilane (MPTS, 95%, Sigma-Aldrich), or trimethoxy(propyl)silane (PTS, 97%, Sigma-Aldrich) was added into the as-prepared PbI_2 solution. For second-step deposition procedure, the FAI/MABr/MACl solution was prepared by adding 1100 mg FAI, 110 mg MABr and 115 mg MACl in isopropanol (IPA) (anhydrous, 99.5%, Sigma-Aldrich), which was filtered with 0.45 μm PTFE-H syringe filter before use. The perovskite films were fabricated by two-step sequential deposition method in a dry room with relative humidity (RH) of ~2%. The PbI_2 solution was spin-coated on the SnO_2 -coated FTO substrate at 2000 rpm for 50 s. Afterward, the as-prepared 300 μL FAI/MABr/MACl solution was sequentially dripped onto the PbI_2 film, stood for 10 s for the penetration of FAI/MABr/MACl solution and spin-coated at 4000 rpm for 20 s. The film was then annealed at 150 °C for 20 min to form perovskite

phase and promote the cross-linking reaction. The hole transporting solution consisted of 72.3 mg of 2,2',7,7'-tetrakis(*N,N'*-di-*p*-methoxyphenylamine)-9,9'-spirobifluorene (Spiro-MeOTAD), 28.8 μL of 4-*tert*-butylpyridine (96%, Sigma-Aldrich) and 17.5 μL of lithium bis(trifluoromethanesulfonyl)imide (Li-TFSI) (99.95%, Aldrich, 520 mg/mL in acetonitrile) solution dissolved in 1 mL of chlorobenzene (anhydrous, 99.8%, Sigma-Aldrich). A spiro-MeOTAD layer was formed on the perovskite layer by spin-coating at 3000 rpm for 30 s. Finally, ~ 100 nm of Au electrode was thermally evaporated on the spiro-MeOTAD film at a constant evaporation rate of 0.3 $\text{\AA}/\text{s}$ in a vacuum chamber with a base pressure of 2×10^{-8} Torr.

Characterization. Photocurrent density-voltage (J - V) curves of PSCs were measured by using 2400 source meter and solar simulator under simulated one sun illumination (AM 1.5 G, 100 mW/cm^2) equipped with 450 W Xenon lamp (Newport 6279 NS). The light intensity was adjusted with an NREL-calibrated Si solar cell. A metal mask with an aperture area of 0.125 cm^2 was superimposed on top of the device to define the active area during the measurement. The UV-vis absorption spectra were obtained using UV-vis spectrometer (Lambda 45, Perkin Elmer). Steady-state photoluminescence (SSPL) and time-resolved PL (TRPL) spectra measurement were carried out using a fluorescence lifetime spectrometer (QuantaaurusTauC11367-12, HAMAMATSU) with the excitation of a 464 nm laser (PLP-10, HAMAMATSU) pulsed at a frequency of 10 MHz for SSPL and 500 KHz for TRPL. Time-correlated single-photon counting (TCSPC) technique was applied to measure the spontaneous photoluminescence decay. X-ray photoelectron spectroscopy (XPS) data were obtained using ESCALAB 250 XPS system (Thermo Fisher Scientific) with Al $K\alpha$ X-ray radiation (1486.6 eV). Atomic force microscopy (AFM) images were obtained using a XE-70 (Park Systems Corp., Korea). Crystal structures of perovskite films were characterized by X-ray diffraction (XRD) (Rigaku D/Max 2200), using Ni-filtered Cu $K\alpha_1$ radiation ($\lambda=1.54184$ \AA). Top-view and cross-sectional scanning electron microscopy (SEM) images were obtained from a field-emission SEM (Jeol JSM7000F). Fourier transform infrared (FTIR) spectra were recorded in a Varian FTIR spectrophotometer (FTS800). High-resolution

transmission electron microscope (HRTEM) was performed on JEOL JEM-2010 with accelerating voltage of 200 KV and a beam current at 105 μ A. The sample was prepared by scraping the MPTS perovskite thin film from glass and ultrasonically dispersed in anhydrous chlorobenzene solvent for 30 min. After that, we dropped 10 μ l of the as-prepared solution on a copper-200 mesh on microgrid for the test of HRTEM. Impedance was measured in the dark using an Autolab 302B in the frequency range of 0.1 Hz to 1 MHz. Incident photon-to-current conversion efficiency (IPCE) was obtained by using a quantum efficiency system (IQE 200B, Newport) in AC mode. Photoelectron spectroscopy (PESA) measurements were carried out for estimation of the highest occupied molecular orbital (HOMO) levels. An incident radiation energy was scanned between 4.5 and 6.2 eV in air.

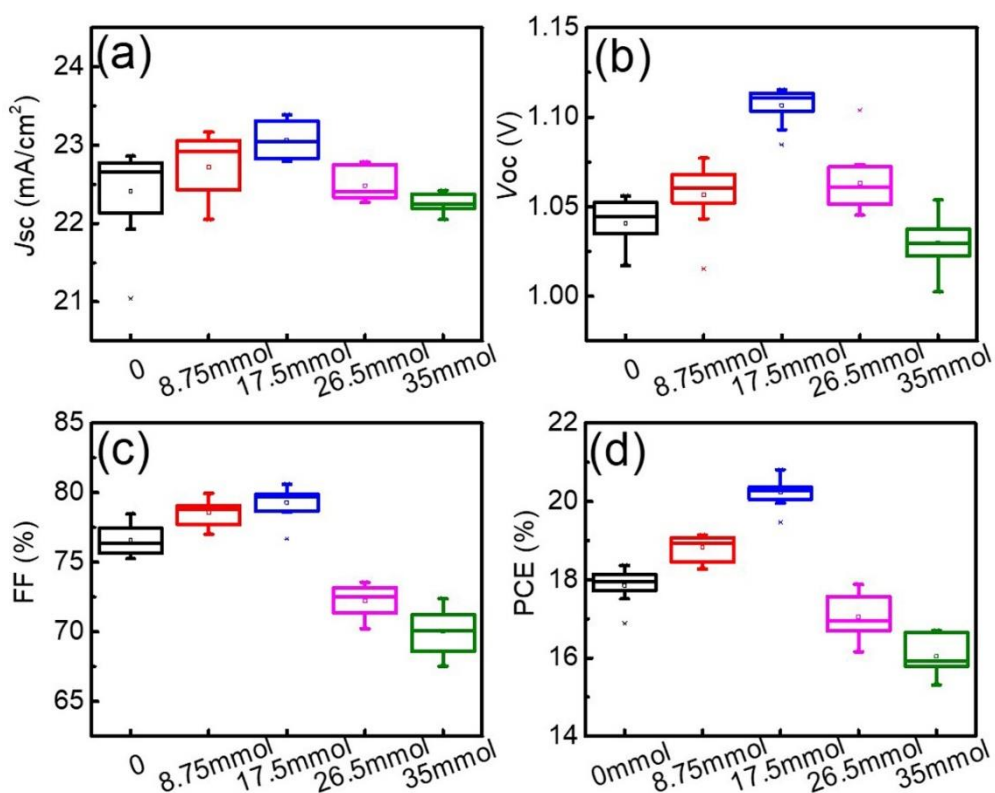


Figure S1. Statistic (a) current density (J_{sc}), (b) open circuit voltage (V_{oc}), (c) fill factor (FF) and (d) power conversion efficiency (PCE) of devices depending on the concentration of MPTS. The statistical data were obtained from 10 separate cells for each concentration.

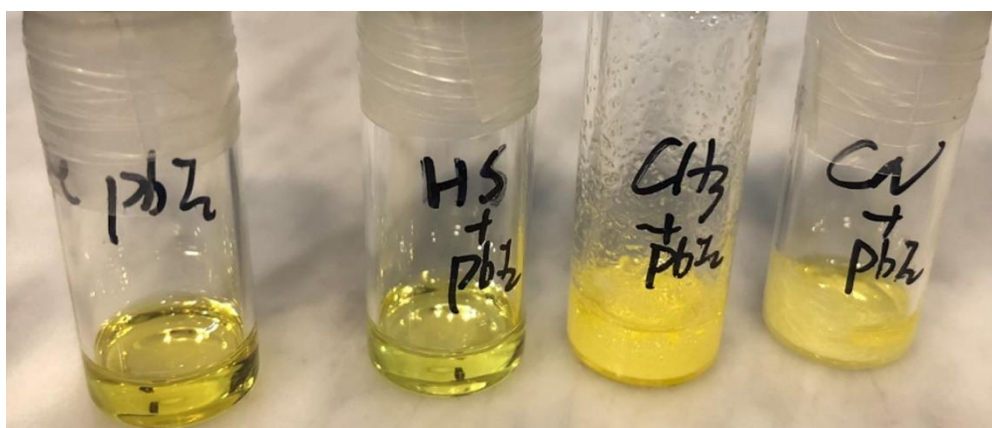


Figure S2. The image of PbI_2 dissolved in DMF solutions with and without crosslinking agents (pure PbI_2 , MPTS(HS+ PbI_2), PTS(CH_3 + PbI_2) and CPTS (CN+ PbI_2) from left to right). The molar ratio between the PbI_2 and crosslinking agents is enhanced to 10:1 test the solubility of PbI_2 in the precursor solution. After 2 h, the precipitates were found in PTS and CPTS solutions. The addition of the PTS and CPTS reduce the solubility of PbI_2 in DMF.

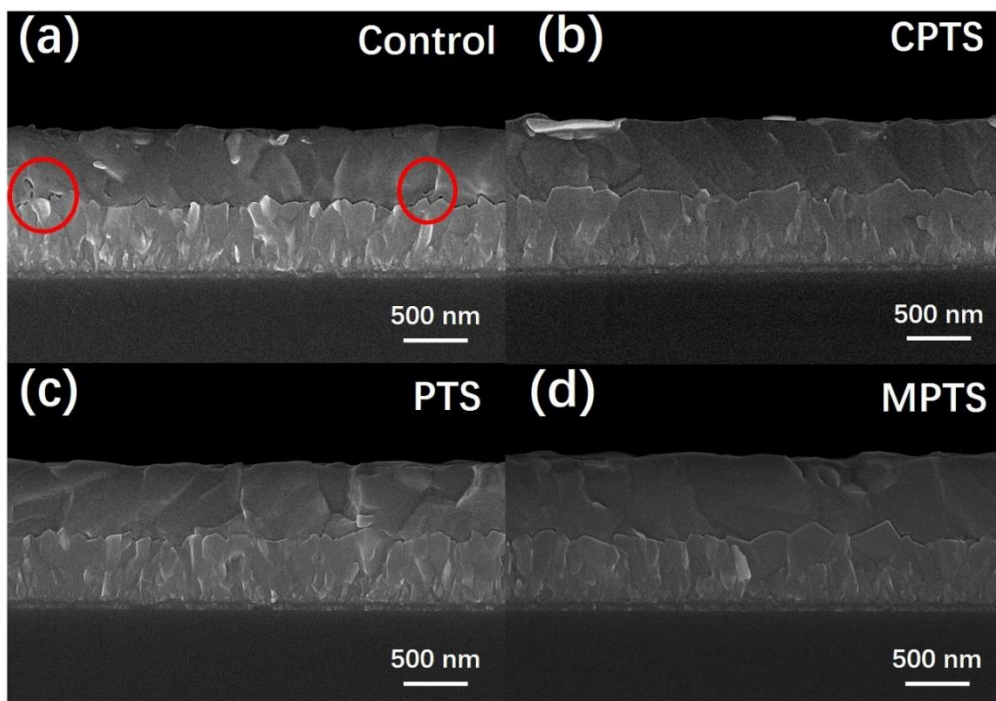


Figure S3. Cross-sectional SEM images of FTO/SnO₂/perovskite, where perovskite film was prepared based on (a) control, (b) CPTS, (c) PTS and (d) MPTS.

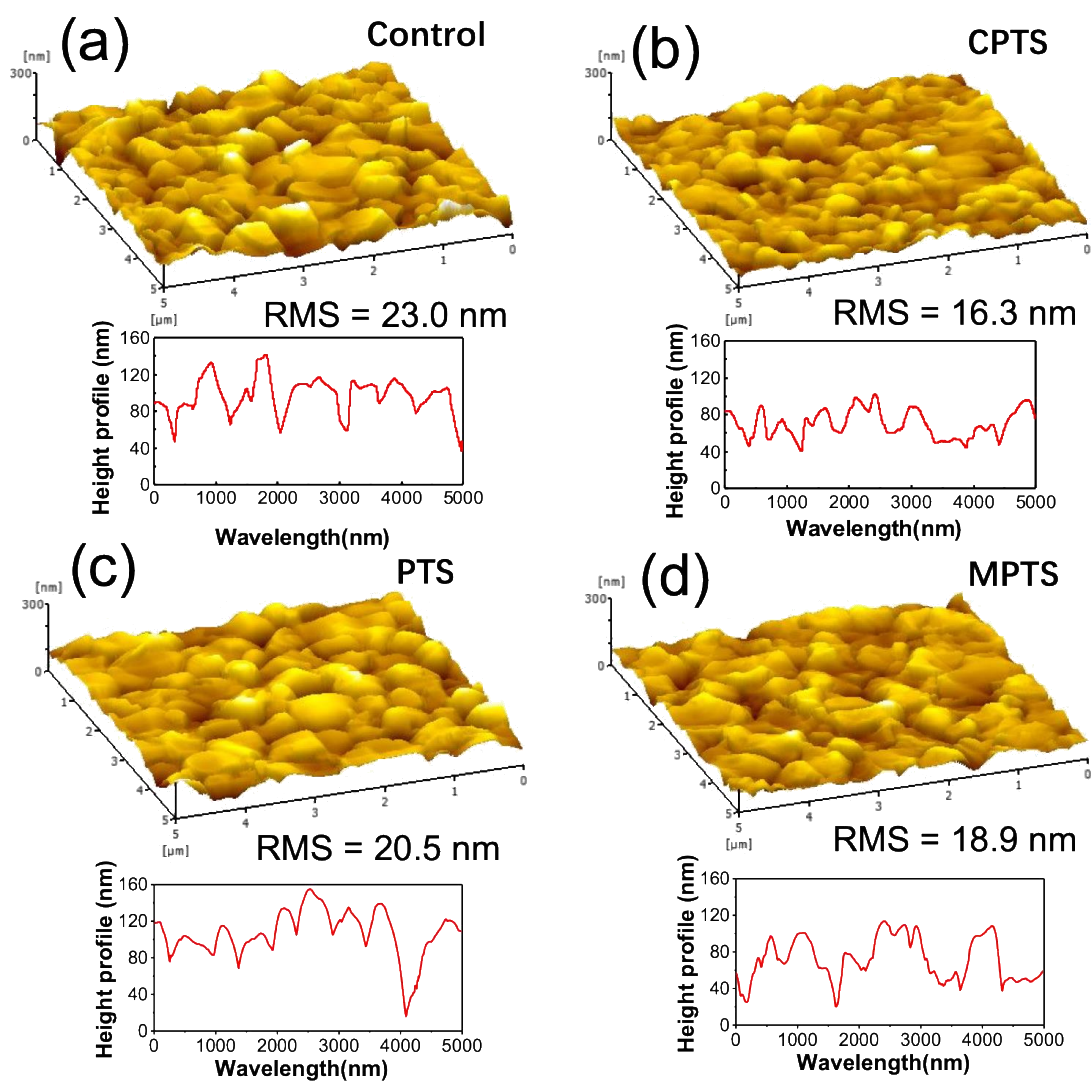


Figure S4. The 3D AFM and height line profile of perovskite films based on (a) control, (b) CPTS, (c) PTS and (d) MPTS.

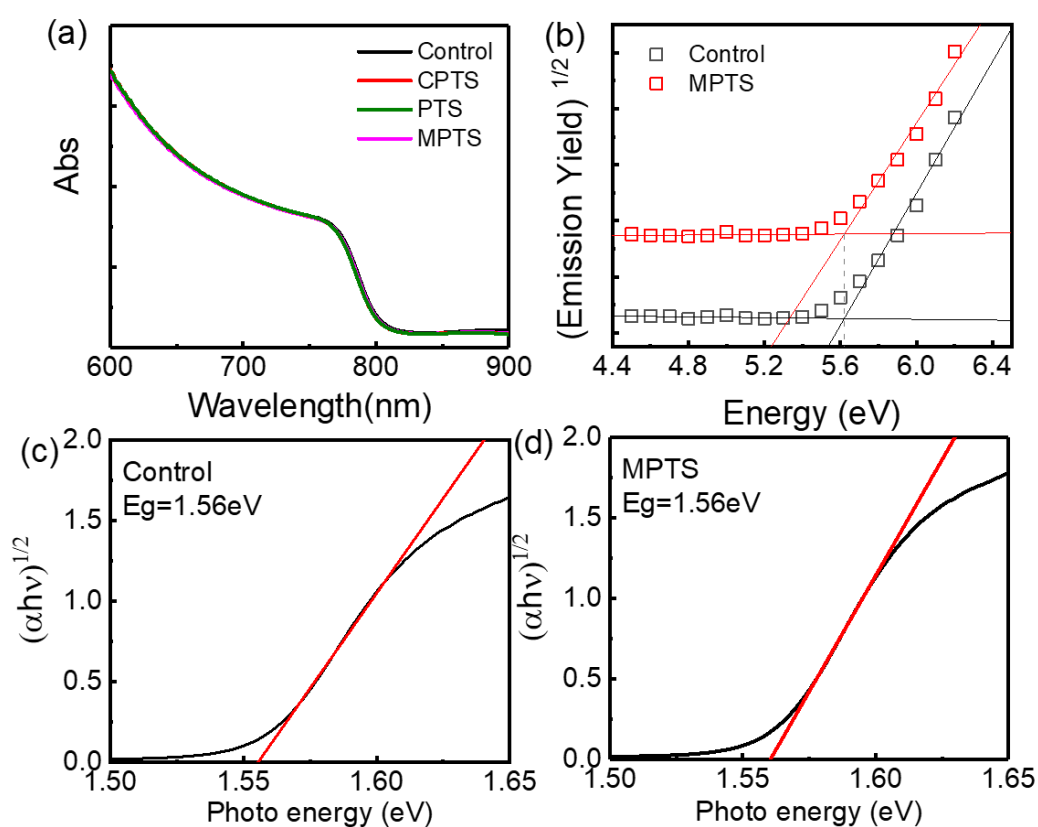


Figure S5. (a) UV-vis absorption spectra of perovskite films prepared on FTO/SnO₂ substrates with CPTS, PTS, MPTS and control films. (b) Photoelectron spectroscopy in air (PESA) spectra of control and MPTS film. Optical bandgap estimated based on Tauc plot for (c) control film and (d) MPTS film.

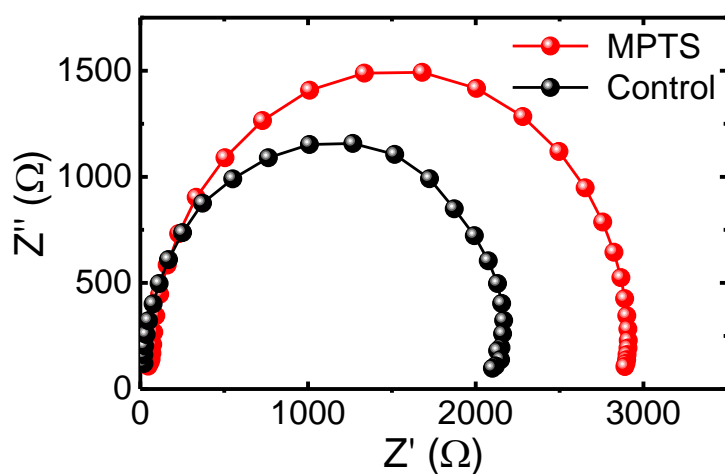


Figure S6 Nyquist plot of perovskite solar cells without (black) and with MPTS (red).

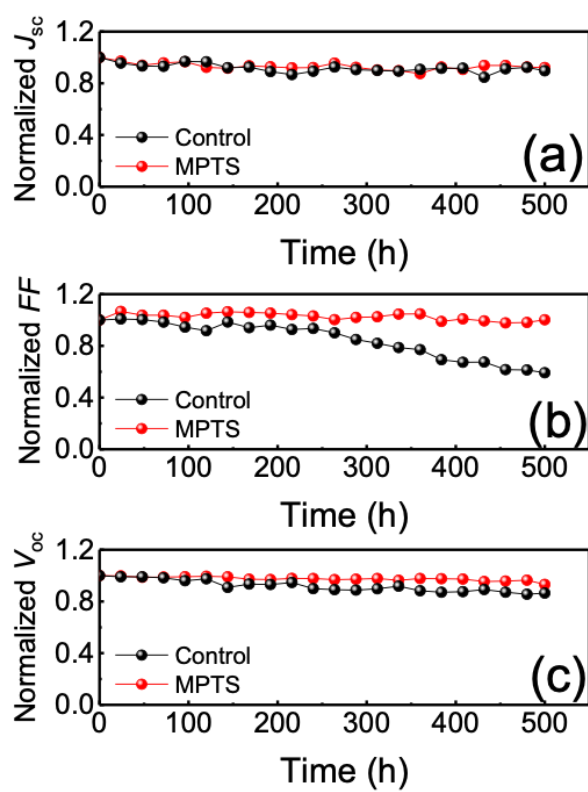


Figure S7. The degradation of photovoltaic parameters (a) J_{sc} , (b) FF and (c) V_{oc} as a function of aging time for control and MPTS devices at a constant temperature of 85°C under ~ 2% humidity condition.

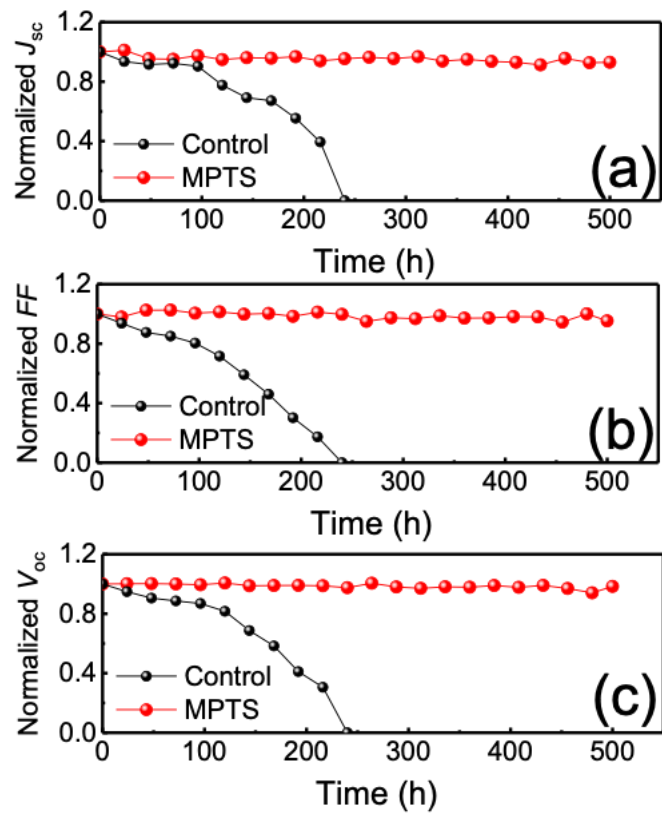


Figure S8. The degradation of photovoltaic parameters (a) J_{sc} , (b) FF and (c) V_{oc} as a function of aging time for control and MPTS devices. The devices were exposed to a relative humidity range of 25% - 45% at room temperature.

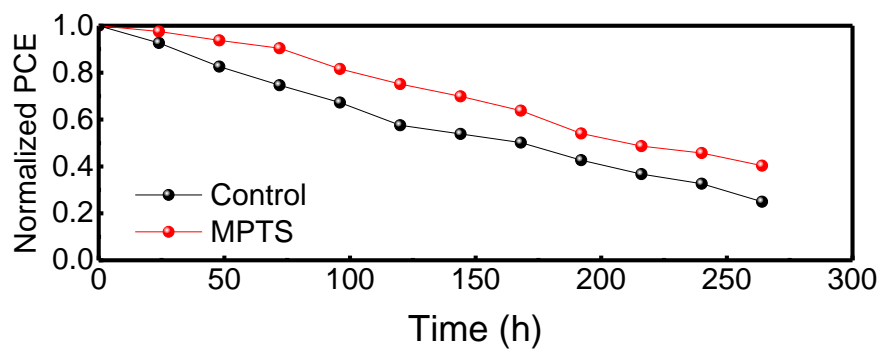


Figure S9. Photo-stability of unencapsulated devices without and with MPTS under one sun illumination at room temperature in the glove box.

Table S1. Summary of best and average photovoltaic parameters (reverse scan) of devices processed with different concentration of MPTS.

MPTS		J_{sc} (mA/cm ²)	V_{oc} (V)	FF (%)	PCE (%)
0mmol	Best	22.25	1.04	79.2	18.4
	Average	22.40±0.26	1.04±0.02	77.1±2.0	17.9±0.37
8.75mmol	Best	22.71	1.07	79.7	19.3
	Average	22.72±0.32	1.05±0.02	78.6±1.0	18.8±0.28
17.5mmol	Best	23.39	1.12	80.0	20.8
	Average	23.06±0.24	1.11±0.01	79.3±1.1	20.2±0.27
26.5mmol	Best	22.157	1.06	75.3	17.88
	Average	22.48±0.21	1.06±0.017	72.2±1.2	17.1±0.55
35mmol	Best	21.72	1.05	74.17	16.98
	Average	22.24±0.13	1.03±0.01	70.0±1.5	16.04±0.48

Table S2. Fitted results of TRPL decay curves in **Figure 5b** using a bi-exponential decay equation of $I(t) = I_0 + A_1 \exp(-t/\tau_1) + A_2 \exp(-t/\tau_2)$, where τ_1 and τ_2 represent fast and slow decay time, respectively. $\tau_{ave} = (A_1\tau_1^2 + A_2\tau_2^2)/(A_1\tau_1 + A_2\tau_2)$.

	Control		CPTS		PTS		MPTS	
	τ_1	τ_2	τ_1	τ_2	τ_1	τ_2	τ_1	τ_2
τ (ns)	6	826	2	499	4	786	8	1070
%	38.9	61.1	64.5	35.5	35.2	64.8	38.9	61.1
τ_{Ave} (ns)	823		495		784		1065	

Table S3. Capacitance (C), V_{TFL} , dielectric constant (ϵ), trap density (n_t), and area (A) of perovskite films fabricated by different crosslinking agents. The ϵ of the perovskite was calculated by the formula of $\epsilon = (C_g L)/(\epsilon_0 A)$. The n_t was calculated through the equation of $n_t = (2\epsilon\epsilon_0 V_{TFL})/(eL^2)$.

Device ID	C ($\times 10^{-8}$ F)	V_{TFL} (V)	ϵ	Area (cm ²)	n_t ($\times 10^{16}$ cm ⁻³)
Control	1.37	0.633	38.5	0.201	1.08
CPTS	1.41	0.777	40.2	0.198	1.38
PTS	1.43	0.619	41.4	0.195	1.13
MPTS	1.31	0.401	36.6	0.202	0.65